Journal of Plant Interactions

ISSN: 1742-9145 (Print) 1742-9153 (Online) Journal homepage: https://www.tandfonline.com/loi/tjpi20

Synchrotron-based FTIR microspectroscopy of chili resistance induced by *Bacillus subtilis* strain D604 against anthracnose disease

Kanjana Thumanu, Darawadee Wongchalee, Mathukorn Sompong, Piyaporn Phansak, Toan Le Thanh, Weravart Namanusart, Kunthika Vechklang, Supaporn Kaewnum & Natthiya Buensanteai

To cite this article: Kanjana Thumanu, Darawadee Wongchalee, Mathukorn Sompong, Piyaporn Phansak, Toan Le Thanh, Weravart Namanusart, Kunthika Vechklang, Supaporn Kaewnum & Natthiya Buensanteai (2017) Synchrotron-based FTIR microspectroscopy of chili resistance induced by *Bacillus subtilis* strain D604 against anthracnose disease, Journal of Plant Interactions, 12:1, 255-263, DOI: 10.1080/17429145.2017.1325523

To link to this article: https://doi.org/10.1080/17429145.2017.1325523

Published online: 25 May 2017.

JOURNAL OF PLANT INTERACTIONS, 2017
VOL. 12, NO. 1, 255–263
https://doi.org/10.1080/17429145.2017.1325523

Taylor & Francis
Taylor & Francis Group

RESEARCH ARTICLE

OPEN ACCESS Check for updates

Synchrotron-based FTIR microspectroscopy of chili resistance induced by *Bacillus subtilis* strain D604 against anthracnose disease

Kanjana Thumanu[a]*, Darawadee Wongchalee[b,c]*, Mathukorn Sompong[b], Piyaporn Phansak[d], Toan Le Thanh[b,e], Weravart Namanusart[f], Kunthika Vechklang[g], Supaporn Kaewnum[c] and Natthiya Buensanteai[b]

[a]Synchrotron Light Research Institute (Public Organization), Nakhon Ratchasima, Thailand; [b]School of Crop Production Technology, Institute of Agricultural Technology, Suranaree University of Technology, Nakhon Ratchasima, Thailand; [c]Bioactive Agro-Industry Co., Ltd, Seang-Sang, Nakhon Ratchasima, Thailand; [d]Division of Biology, Faculty of Science, Nakhon Phanom University, Nakhon Phanom, Thailand; [e]Crop Protection Department, College of Agriculture and Applied Biology, Can Tho University, Can Tho City, Vietnam; [f]Department of Agricultural Technology and Environment, Faculty of Science and Liberal Arts, Rajamangala University of Technology, Nakhon Ratchasima, Thailand; [g]Department of Applied Biology, Faculty of Science and Liberal Arts, Rajamangala University of Technology, Nakhon Ratchasima, Thailand

ABSTRACT

The aim of this study was to determine the resistance mechanisms of chili induced by the *Bacillus subtilis* strain D604 using synchrotron FTIR microspectroscopy (SR-FTIR). In this study, the strain D604 reduced anthracnose disease severity in chili plants by approximately 31.10%. The SR-FTIR spectral changes from the epidermis and mesophyll leaf tissue revealed higher integral areas for the C=O ester from lipids, lignin, or pectin (1770–1700 cm^{-1}) as well as polysaccharides (1200–900 cm^{-1}) in the treated samples of D606 and distilled water and then challenge inoculation with chili anthracnose pathogen, *Colletotrichum acutatum*. The secondary structure of the Amide I protein failed to convert from alpha helices (centered at 1650 cm^{-1}) to beta sheets (centered at 1600 cm^{-1}) in the mesophyll of samples not treated with D604. This study suggested that the strain D604 induced resistance against anthracnose pathogen in chili by inducing cellular changes related to defense compounds involved in plant defense mechanism.

ARTICLE HISTORY
Received 23 August 2016
Accepted 27 April 2017

KEYWORDS
SR-Fourier transform infrared; chili anthracnose; *Bacillus subtilis*; biochemical composition; hierarchical cluster analysis (HCA); induced resistance

Introduction

Anthracnose disease, caused by *Colletotrichum* sp., is an important disease of chili in Thailand. *Colletotrichum* is one of the most important plant pathogens worldwide causing the economically important anthracnose disease in a wide range of hosts including cereals, legumes, vegetables, perennial crops, and tree fruits. When chili (*Capsicum* spp.) is severely infected, yield losses can reach up to 50% (Pakdeevaraporn et al. 2005). In recent years, conventional management of anthracnose in chili has relied on aggressive chemical approaches that are vulnerable to the development of fungicide resistance and leave chemical residues harmful to human health and the environment (Buensanteai et al. 2009). An alternative control method is the use of beneficial microbes with antagonism against the causal agent of anthracnose. *Bacillus* sp. is widely used commercially to control plant pathogens and to enhance plant growth. In addition to directly affecting plant growth and development through the production of plant growth regulators, *Bacillus* sp. can colonize plant roots and trigger plants to produce growth-promoting biomolecules. The plant growth-promoting rhizobacteria (PGPRs), *Bacillus* sp., have been shown to promote growth and induce systemic resistance (ISR) in several economic crops such as soybean, corn, rice, cassava, Chinese kale, and cauliflower against multiple pathogens (Prathuangwong & Buensanteai 2007; Buensanteai et al. 2009, 2012). Various reports indicate the potential for PGPRs to provide control of diseases in chili pepper. A mixture of *B. megaterium* SBK5.7 and *Bacillus* sp. SPT41.1.3 effectively reduced the severity of anthracnose on seeds by 41.90% when compared to controls under field conditions. A cell suspension of *B. licheniformis* BFP011 also reduced the disease severity of *C. capsici* by more than 30% (Plodpai et al. 2008; Ashwini & Srividya 2014).

Resistance inducers have been extensively evaluated as a means to control plant diseases based on the induced resistance (IR) concept including ISR and systemic acquired resistance (Ryu et al. 2004; Buensanteai et al. 2009; Ashwini & Srividya 2014). IR is part of the plant innate defense system that confers long-lasting protection against a broad range of pathogens (Kloepper et al. 2004, Ryu et al. 2004; Conrath et al. 2006). Once resistance is induced, the plant acquires enhanced defensive capacity against subsequent infection by pathogens. IR requires a signal molecule and is associated with the production and the accumulation of pathogenesis-related (PR) proteins (Buensanteai et al. 2009). The inducers can be both biotic and abiotic. Among the biotic inducers, PGPRs, including *Bacillus*, have been extensively evaluated against several diseases (Kloepper et al. 2004; Buensanteai et al. 2009). Their application has been registered by many governments for the protection of a diverse set of crops (Conrath et al. 2006; Buensanteai et al. 2008). Mechanisms of *Bacillus*-IR include rising cytosolic H^+ and Ca^{2+}, activation of MAP-kinases, callose deposition, lignin, hypersensitive response, and synthesis of compounds including salicylic acid (SA), jasmonic acid, phytoalexins, and PR proteins (Conrath et al. 2006; Buensanteai et al. 2009). The defense mechanisms induced by the strain D604 against anthracnose

CONTACT Natthiya Buensanteai natthiya@sut.ac.th
*The first and second authors equally contributed to this work.

disease in chili remain a gap in current knowledge. Activation of plant defense mechanisms are traditionally observed by monitoring changes in cellular components using enzymatic analysis and histological assay (Buensanteai et al. 2009). However, these methods rely on the use of bulk samples resulting in averaging of the intrinsic inter-tissue and cellular heterogeneity. Therefore, an accurate understanding of the cellular and biochemical changes associated with *Bacilli* in chili can be achieved by use of synchrotron-based FTIR microspectroscopy, a technique capable of resolving biochemical changes at the plant cellular level (Thumanu et al. 2015).

Synchrotron-based Fourier Transform Infrared (SR-FTIR) microspectroscopy, combined with multivariate data analysis, is used to interpret the interactions between plant microbes and plant pathogens because it is discriminating enough to allow the identification of functional groups of plant cellular components (Kenneth & Lawrence, 2005; Yu 2008; Thumanu et al. 2015). SR-FTIR provides detailed chemical structures and composition of plant tissues based on specific vibration characteristics of chemical functional group of each sample (Dokken & Davis 2005; Wang et al. 2012). Moreover, FTIR microspectroscopy is a nondestructive analytical technique that is less time consuming and cheaper than the present 'gold standard' methods, providing unique molecular chemical information based on the FTIR spectrum (Yu 2005). For example, the amide I protein band that contains vibrations of the peptide bond containing C=O (80%) and N–H stretching (20%), appearing between 1700 and 1600 cm^{-1} can provide information about changes in protein secondary structure. The carbohydrate fingerprint region (1200–800 cm^{-1}) of the FTIR spectra from cells and tissues is obtained via vibrations of C–O bonds present in the C–O–C bonds of polysaccharides, cellulose, hemicellulose, and proteins (Thumanu et al. 2015). Application of FTIR microspectroscopy to identify the chemical structure of plant secondary metabolites has become increasingly important in the study of interactions between plant pathogens and plant microbes (Thumanu et al. 2015). The objective of this study was to apply SR-FTIR microspectroscopy to define tissues within chili leaf sections and to detect biochemical changes in chili plants induced by the application of strain D604 and *Colletotrichum acutatum* that can be associated with resistance mechanisms.

Material and methods

Bacterial strain and culture conditions

The PGPRs, *Bacillus subtilis* strain D604, from stock culture at the Plant Pathology and Biopesticide Laboratory, Suranaree University of Technology, Thailand, stored in nutrient broth with 10% glycerol at −80°C, were retrieved by streaking them from nutrient broth onto Nutrient Glucose Agar at 28 ± 2°C for 48 h. All the bacterial cultures were propagated in 500 mL of nutrient broth containing 2% glucose (NGB) culture medium for 48 h at 28 ± 2°C with constant shaking at 180 rpm. The cultures were suspended in sterile distilled water and the density of the suspension was adjusted to 10^8 cfu mL^{-1} based on optical density (OD of 0.2 at 600 nm) (Buensanteai et al. 2008). A portion of the cell suspension was used in experiments in live form.

Colletotrichum strain and culture conditions

C. acutatum was provided by potato dextrose agar stock culture of Plant Pathology Laboratory, Khon Kaen University, Thailand. The excess traces of NaOCl on the tissue were removed by washing 2 times in sterile distilled water and then transferred aseptically to petri dishes containing Water Agar medium. The inoculated petri dishes were then incubated at 25°C. Growth of the causal fungus was observed periodically for 2 days. The pure fungal colonies that developed from these infected tissues were then transferred onto Half Potato Dextrose Agar (HPDA) plates and maintained in the HPDA slants for the experiments.

Plant materials, treatment, and disease assessment

The greenhouse experiment was conducted using the *B. subtilis* strain D604 to examine IR of chili to anthracnose disease infection. Seeds of chili (*Capsicum annuum*) cv. Super Hot were surface-disinfested by treatment with 95% ethanol (v/v) for 2 min, followed by soaking in 20% commercial bleach (v/v) for 20 min. The seeds were then washed with sterile distilled water 5 times in order to remove the bleach. Before planting, 5 g of chili seeds were mixed thoroughly with 5 mL of a liquid treatment. The three treatments of this experiment included (1) seed treatment and foliar spray containing the strain D604 (2) positive chemical control: carbendazim 20 g/20 L water 3) negative control: water. The chili seeds treated with each treatment were planted in pots (30 cm diameter) containing soil and mixed fertilizer. There were 10 pots per replication, and each treatment was replicated 4 times with one seed planted per pot. The pots were watered daily and supplemented with fertilizer every week. Pots were kept in a greenhouse with a 12-h photoperiod (25°C and 60–75% relative humidity during the light period, 15°C and >93% relative humidity during the dark period). At 14, 21, and 28 days after planting, each plant received a foliar spray of each treatment (slightly modified from Prathuangwong & Buensanteai 2007; Buensanteai et al. 2009).

The conidial suspensions of *C. acutatum* were collected by scraping the colony surface with a sterile scalpel and 10 mL of sterile distilled water, after which they were filtered through four layers of cheesecloth to remove any mycelial debris, and spores were counted with a hemocytometer and adjusted to 1×10^6 conidia/mL. The chili plants were then inoculated according to the method described by Oh et al., with minor modifications. The control plants were inoculated with sterilized water. For the disease assessment, suspensions of conidia and microbial cells of *C. acutatum* in 0.04% Tween 80 were sprayed onto six seedlings of chili plants until it ran off (5 mL/seedling). Plants were kept in the greenhouse for 12 h before and after inoculation to maintain high humidity and facilitate infection. Chili plants were scored as (1) uninfected; (2) 1/3 of the leaves infected; (3) 2/3 of the leaves infected; or (4) dead. The control treated plants with or without fungal pathogen inoculation were collected at the same intervals. The chili anthracnose disease severities were recorded at 7 days after inoculation, using the scale slightly modified from Ashwini and Srividya (2014) for assessing chili anthracnose under a greenhouse condition as follows: 0 = no infection; 1 = 1–25% infection; 2 = 26–50% infection; 3 = 51–75% infection; and 4 = 76–100% infection on the

chili leaves regions. Percentage of disease severity was calculated using the formula slightly modified by Ashwini and Srividya (2014) as follows: disease severity (DS, %) = [Sum of all numerical ratings/(Total number of leaves graded × Maximum grade)] × 100. The reduction of disease severity for treated chili was calculated using the formula as follows: reduction on disease severity = [(DS of non-treated control treatment − DS of *Bacillus*-treated treatment)/DS of non-treated control treatment] × 100. The experiment was performed three times. For statistical analyses, analysis of variance was determined according to Duncan's Multiple Range Test at $p < .05$ by using SPSS version 14.

Synchrotron-based FTIR microspectroscopy

Sample preparation for FTIR microspectroscopy analysis

The treated chili leaf tissues were embedded in OCT compound (Tissue-Trek, Electron Microscopy Sciences, Hatfield, PA), and snap-frozen in liquid N2. Then, the samples were transferred to a −80°C freezer and stored until cryo-sectioning. After that, the sample was cut transversely about 7 microns thick using a cryostat (Leica 3050 S, Germany) and put on infrared transparent BaF2 windows (13 × 2 mm) for infrared microspectroscopy.

FTIR microspectroscopy analysis

Spectra data were collected at an infrared microspectroscopy beamline (BL4.1 IR Spectroscopy and Imaging) at the Synchrotron Light Research Institute (SLRI). Spectra were acquired with a Vertex 70 FTIR spectrometer (Bruker Optics, Ettlingen, Germany) coupled with an IR microscope (Hyperion 2000, Bruker) with an MCT detector cooled with liquid nitrogen over the measurement range from 4000 to 800 cm^{-1}. The microscope was connected to a software-controlled microscope stage and placed in a specially designed box that was purged by dry air. The measurements were performed in the mapping mode, using an aperture size of 10 × 10 μm with a spectral resolution of 4 cm^{-1}, with 64 scans co-added. Spectral acquisition and instrument control were performed using OPUS 7.2 (Bruker Optics Ltd, Ettlingen, Germany) software and analyzed by CytoSpec software.

Table 1. Efficacy of PGPR, *Bacillus subtilis* strain D604 on severity and reduction of anthracnose disease in chili cv. Super Hot caused by *Colletotrichum acutatum* in a greenhouse condition.

Treatment[a]	Disease severity (%)[b]	Disease reduction (%)[c]
D604	35.60ab	31.10ab
Carbendazim	31.62b	38.71a
ddH2O	51.67a	0
C.V. (%)	12.11	

[a]Chili leaves were challenged with *C. acutatum*, or sterile distilled water for 7 days after foliar treatment with the strain D604, carbendazim and sterile distilled water.

[b]Disease severity was evaluated 7 days after challenge with *C. acutatum* or sterile distilled water. Each value represents a mean of three replicate plants with two leaves per plant. Mean in the column followed by the same letter is not significantly different according to the LSD test ($\alpha = 0.05$).

[c]The disease score included: 0 = no infection; 1 = 1–25% infection; 2 = 26–50% infection; 3 = 51–75% infection; and 4 = 76–100% infection on the chili leaves regions. Percentage of disease severity was calculated using the formula reported by Ji et al. as follows: disease severity (DS, %) = [Sum of all numerical ratings/(Total number of leaves graded × Maximum grade)] × 100. The reduction of treated rice on disease severity was calculated using the formula as follows: reduction in disease severity = [(DS of non-treated control treatment – DS of *Bacillus*-treated treatment)/DS of non-treated control treatment] × 100.

Data processing for image analysis

IR imaging of the leaf tissue was constructed and analyzed using Cytospec 1.3.4 (Cytospec Inc., NY, USA). The spectra were converted to the second derivative, using 9 smoothing points, and vector normalized to normalize for the effects of differing sample thickness. The image construction was performed using the univariate mode which generates output based on peak intensity, peak area, or peak ratio to yield, commonly referred to as chemical maps or function group maps. Hierarchical clustering analysis (HCA) of the FTIR data was performed to distinguish the different biochemical components of the leaf tissue over spectral ranges of 3000–2800 cm^{-1} and 1800–900 cm^{-1}. The chemical images for HCA were acquired from SR-FTIR mapping at 10 × 10 μm over an area of 110 × 120 μm for the control group and 80 × 210 μm for the treated chili plant. The individual 2D cluster maps were recorded as an image file with a unique color to assign each cluster.

Multivariate data analysis

The spectra from each cluster of epidermis and mesophyll leaf tissue from the control and the treated chili plant were analyzed using principle cluster analysis (PCA) to distinguish different biochemical components of each tissue. The spectra were processed using second derivative and vector normalized by the Savitzky–Golay method (3rd polynomial, 13 smoothing points) using the UnscramblerX 10.1 software. (CAMO, Norway).

Results and discussion

The PGPR, *B. subtilis* strain D604, effectively induced resistance of chili against *C. acutatum* under greenhouse conditions (Figure 1). The results showed that anthracnose occurrence in chili was affected by seed and foliage treatment of the strain D604 in the greenhouse. The strain D604 significantly reduced anthracnose disease severity by approximately 31.10% on foliage of chili, confirming that induction of systemic resistance had occured (Table 1). Furthermore, the strain D604-treated plants showed an increase in chili fresh yield when compared with the fungal pathogen-inoculated controls (data not shown). Moreover, the results indicated that foliar treatment with the chemical fungicide, carbendazim, reduced the severity of anthracnose in the chili foliage by 38.21%. Both fungicide and PGPR treatments resulted in disease severities that were significantly lower than that of the non-treated control treatment (Table 1).

In order to investigate the effects of *B. subtilis* strain D604 on the defense response of chili, the biochemical and cellular compositions of chili leaves were evaluated. Table 2 identifies the bands that correspond with major cellular constituents such as proteins, lipids, and polysaccharides. The main advantage of SR-FTIR mapping is its ability to detect plant biochemical components at high spatial resolution and high S/N ratio using a small aperture size. Chemical imaging of functional groups from chili leaf analyzed by SR-FTIR microspectroscopy is shown in Figure 1(a,b). The IR images display the integrated area of Amide I protein in the spectral range of 1700–1600 cm^{-1}. Absorbance intensities from chemical mapping were proportional to color change: blue (the lowest) < green < yellow < red (the highest). In order to compare spectral changes of transverse leaf sections of chili pepper, HCA was applied to distinguish spectra based on similarities and

Table 2. IR band assignment for plant tissue.

Frequency range (cm^{-1})	Functional groups	References
1730	C=O ester from lignin and hemicellulose/ Pectin	Yu (2005)
1650	Amide I band (C=O stretch (80%), C–N stretch (10%), N–H bending (10%)	Yu (2005, 2008)
1550	Amide II (N–H bend (60%), C–N stretch (40%)	Yu (2005, 2008)
1510	C=C aromatic ring from lignin	
1450	Asymmetric CH_2 and CH_3 bending from lipids, protein, lignin	
1370	Symmetric CH_2 and CH_3 bending from lipids, protein, lignin	
1246	C–O stretching from hemicelluloses and lignin	
1200–1000	Mainly C–O–C of polysaccharides; very complex and depends upon contributions from polysaccharides, cellulose, hemicellulose, and pectins	
1105	C–O–C glycosidic ether mainly hemicellulose	Wang et al. (2012)
1155	C–C ring cellulose	Wang et al. (2012)
1022, 1047, 1080	C–C, C–O stretching from carbohydrates	Wang et al. (2012)

differences of the biochemical components in the plant tissue. The spectral differences between treatments demonstrated that there were differences in the concentrations of lipids, proteins, lignins, and polysaccharides (Figure 2(a)). The HCA analysis of spectra from each cluster was separated based on similarity to and dissimilarity from each biochemical functional group. For the control plants, our results showed that the epidermal tissue was grouped in clusters 1, 3, and 5. The mesophyll tissue was represented in cluster 2 and is coded by blue in the color index. The averaged spectra from each cluster were shown in Figure 2(b,c). The spectra of chili leaf tissue treated with the strain D604 were divided into mesophyll and epidermal subgroups, with the mesophyll tissue assigned to clusters 2 and 5 and the epidermal tissue assigned to clusters 3 and 4 (Figure 3(a–c)).

Multivariate analysis was used to compare the biochemical differences across tissue types and treatments. There are two types of information extracted from this method: first, the visualization of clustering of similar spectra within datasets in scores plots; additionally, the identification of variables of spectral bands representing various biochemical molecular groups within the samples in loadings plots to explain the clustering observed in the score plots. The complex FTIR spectra can resolve the largest spectra variable within the leaf tissue. The PCA explains spectral changes of epidermis tissue compared between the control and D604-treated groups (Figure 4(a,b)). Additionally, the analysis demonstrated that the PC1 and PC2 consistently provide the best clustering of the two groups. The PCA score plot was sufficient to group separately the control and the treated groups, which was explained by 50% PC1 and 31% PC2, respectively. The high positive loading from PC1 at 1625 and 1166 cm^{-1} corresponded with the positive score plot from the control epidermis group. In contrast, the high negative loading from the PC1 at 1733, 1450, 1240, and 1097 cm^{-1} corresponded with the negative score plot from the treated epidermis group (Figure 4(a,b)). The PCA score plot from the control mesophyll tissue was associated with the positive

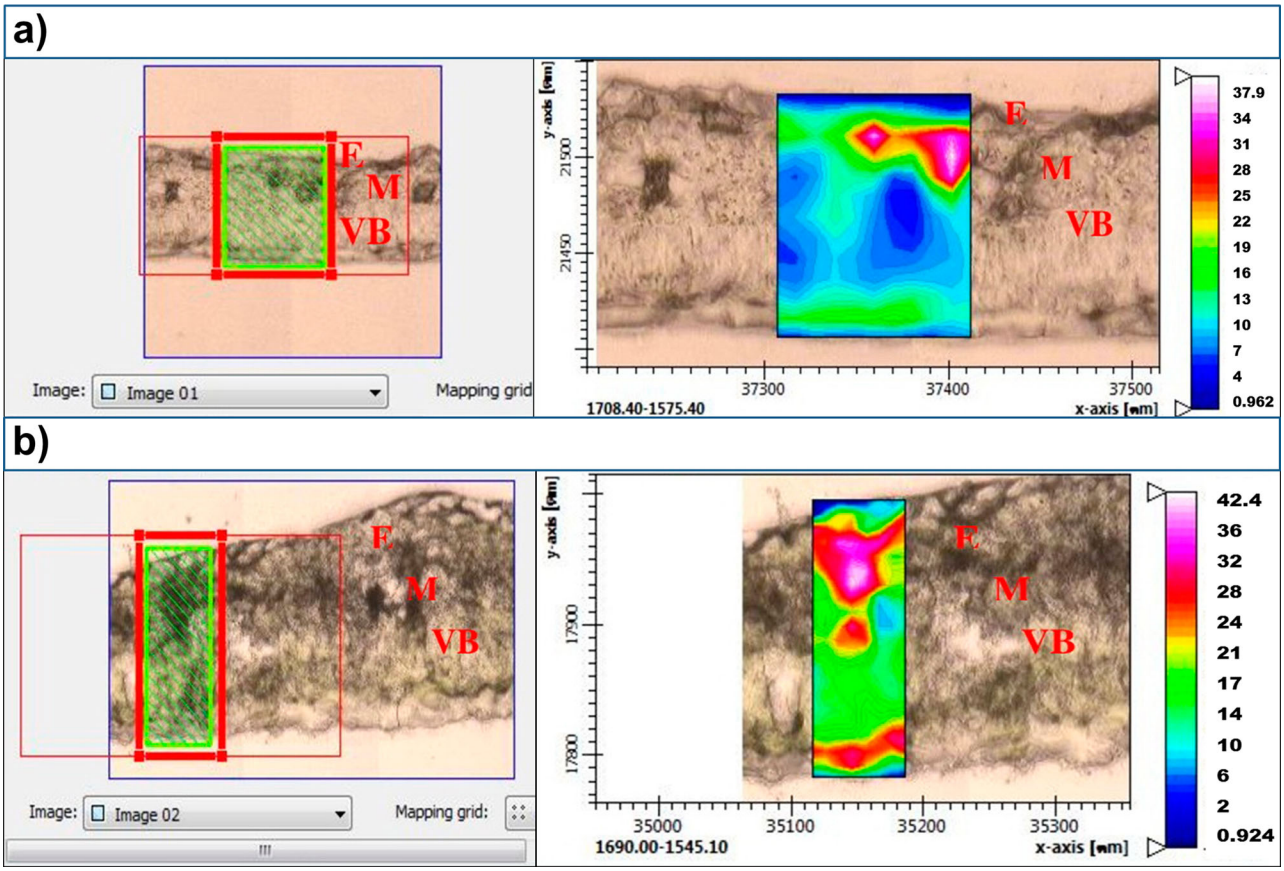

Figure 1. Functional group area maps obtained under the spectral region between 1700 and 1580 cm^{-1} of a part of a transverse leaf section from chili (a) compared with chili leaf tissue induced by the strain D604, and (b) The measurement was performed by point to point mapping with aperture setting at 10 × 10 µm square aperture, 4 cm^{-1} 64 scans using SR-IR microspectroscopy over an area of 110 × 120 µm for the control group and 80 × 210 µm for the treated group.

Notes: E: Epidermis, M: Mesophyll, VB: Vascular bundle.

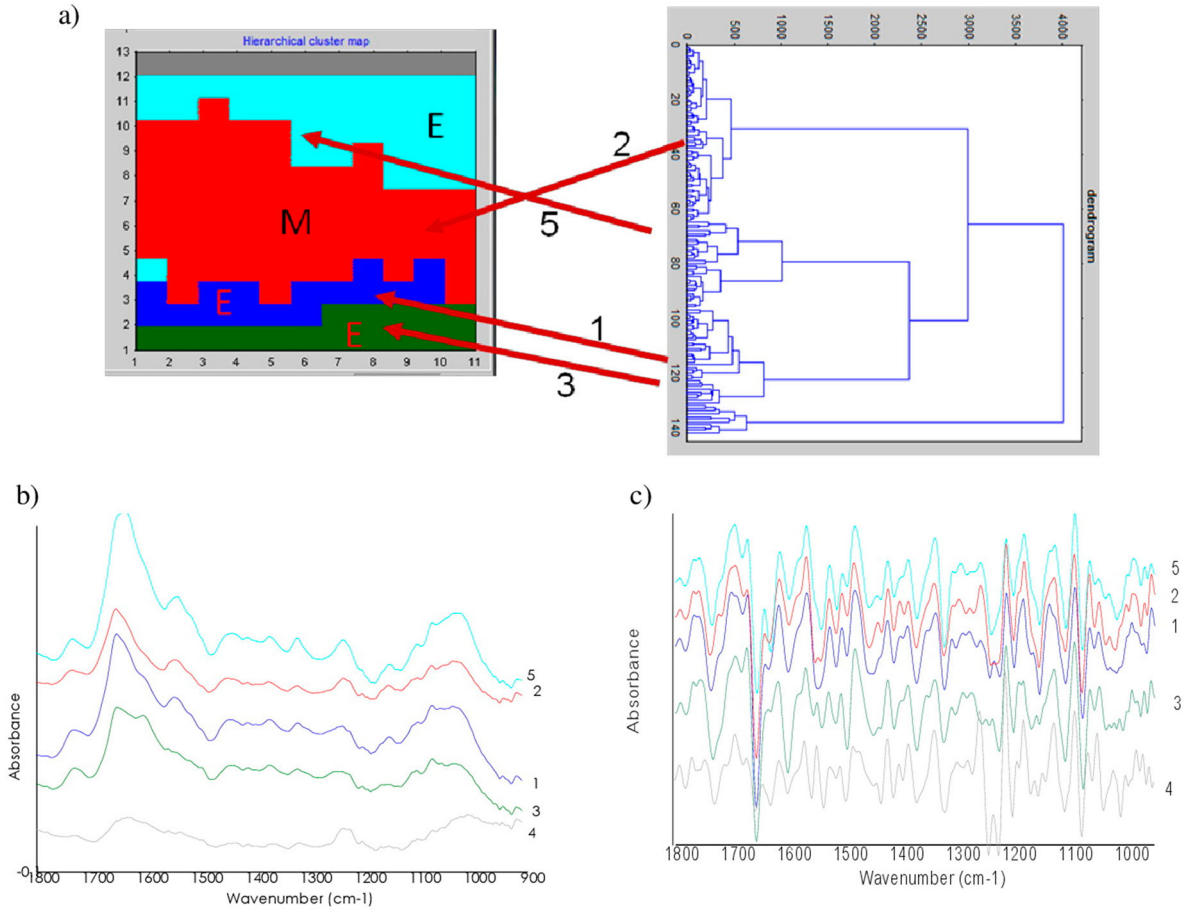

Figure 2. SR-FTIR mapping of a non-treated chili leaf and challenge inoculation with *C. acutatum* (control group) (a) 2D HCA map performed using five clusters on the range of 1800–900 cm^{-1}, different clusters are encoded by different colors, (b) Representative original average spectra of the spectra cluster, and (c) Representative second derivative of the spectra cluster. Mesophyll (cluster average spectra 2), epidermis (cluster 1, 3, and 5).

loading plot at 1654, 1546, and 1234 cm^{-1}. The first two PC explained 88% of the total variance in the data set with 76% and 12% of the total variance explained by PC1 and PC2, respectively. The positive loading plot at 1654, 1546, and 1230 cm^{-1} corresponded with the positive score plot of the control group (Figure 4(c,d)). The high level of alpha helix secondary structure for protein was only found in the treated group. The separation along PC1 and PC2 can be explained by the total variance of 76% from PC1 and 12% from PC2.

In order to visualize differences in the spectra from control and treated groups, the mean integrated areas were calculated. We observed differences in spectra between the epidermal and mesophyll groups (Figure 5(a,b)). Spectral changes for the Amide I protein (1700–1600 cm^{-1}), lipid or pectin (1740–1700 cm^{-1}), CH bending (1480–1300 cm^{-1}), C–O–C hemicellulose and cellulose (1200–1250 cm^{-1}) and polysaccharide region (1200–900 cm^{-1}) were observed (Table 2). In order to compare the difference between these two groups, the mean integrated area of original spectra for each functional group was calculated (Tables 3 and 4). The absorbance in the spectral range from 1650 to 1659 cm^{-1} was associated with the presence of alpha helix structure. Treated chili plants displayed a decrease of alpha helix structure (centered at 1656 cm^{-1}) accompanied by an increase in beta sheet structure (centered at 1600 cm^{-1}) (Figure 5(a)). For the epidermal leaf tissue, we observed differences between the control and the D604-treated groups, revealing higher integral areas of D604-treated chili for the C=O ester from lipids, lignin, or pectin (1770–1700 cm^{-1}) as well as protein Amide I and Amide II (1700–1500 cm^{-1}), polysaccharides (1200–900 cm^{-1}). Additionally, the intensity of the alpha helix secondary structure (centered at 1650 cm^{-1}) of the Amide I protein was decreased in the treated group and changed to beta sheet secondary structure (centered at 1600 cm^{-1}) of Amide I protein (Figure 6(a,b)). These biochemical changes are known to be associated with callose deposition and thickening of the plant cell wall. The intensity of alpha helix secondary protein structures from mesophyll leaf tissue at 1656 cm^{-1} was increased by application of *B. subtilis* strain D604. In addition, the polysaccharide region (1200–900 cm^{-1}) and CH Bending (1480–1300 cm^{-1}) from the mesophyll region was also higher than the control group. These data indicate the trend of biochemical changes in chili after treatment with the strain D604, which indicate the response mechanisms of anthracnose disease infection (Tables 3 and 4).

We applied SR-FTIR microspectroscopy to analyze changes in the biochemical composition of the leaf cells of chili plants induced by *B. subtilis* strain D604 and *C. acutatum*. This technique investigated chili leaf sections at a high spatial resolution and revealed macromolecular differences between control and treated leaves. This technique combined with PCA can be used to resolve chemical structural information related to the various tissue types in the plant leaf cell (Buensanteai et al. 2012; Thumanu et al. 2015). Importantly, PCA enabled the exploration of spectral changes in both the epidermal and mesophyll tissue after treatment with the strain D604. Our results suggest spectral differences

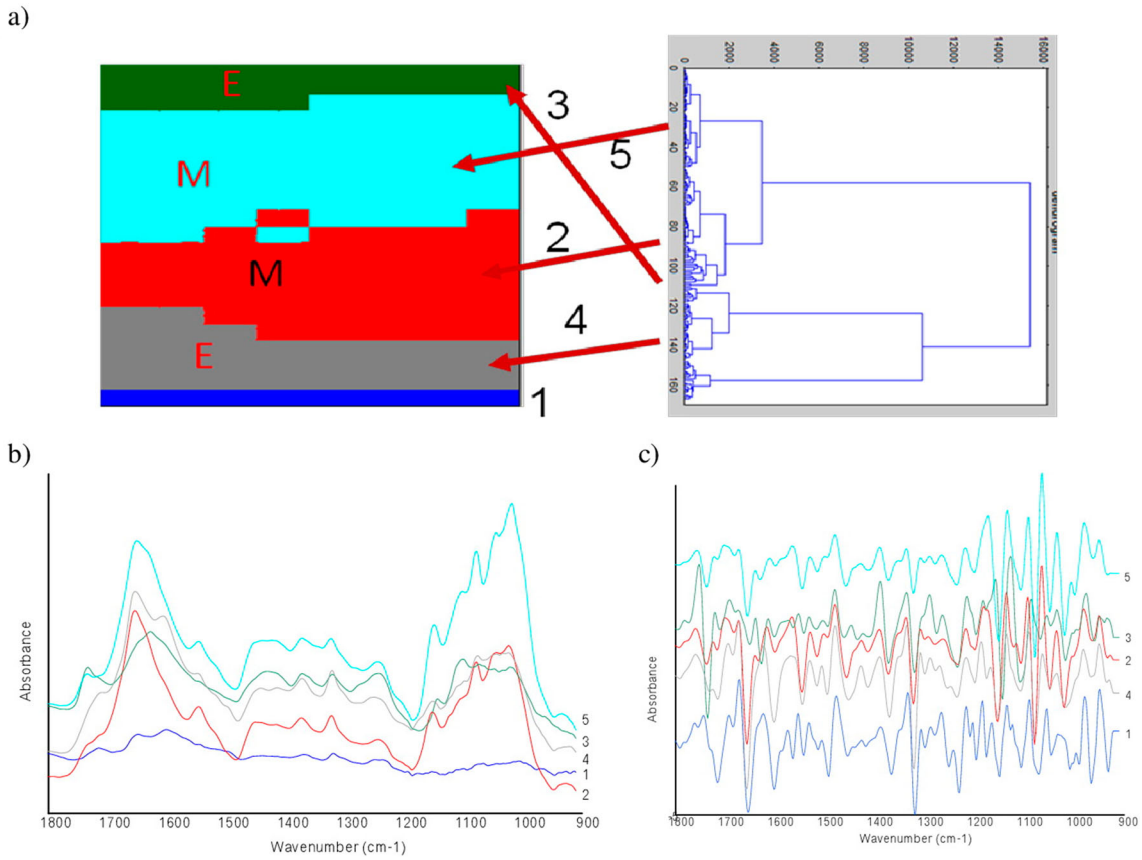

Figure 3. SR-FTIR mapping of chili leaf treated by the strain D604 and challenge inoculation with *C. acutatum* (treated group) (a) 2D HCA map performed using five clusters in the range of 1800–900 cm^{-1}, different clusters are encoded by different colors, (b) Representative original average spectra of the spectra cluster, and (c) Representative second derivative of the spectra cluster. Mesophyll (cluster average spectra 2), epidermis (clusters 1, 3, and 5).

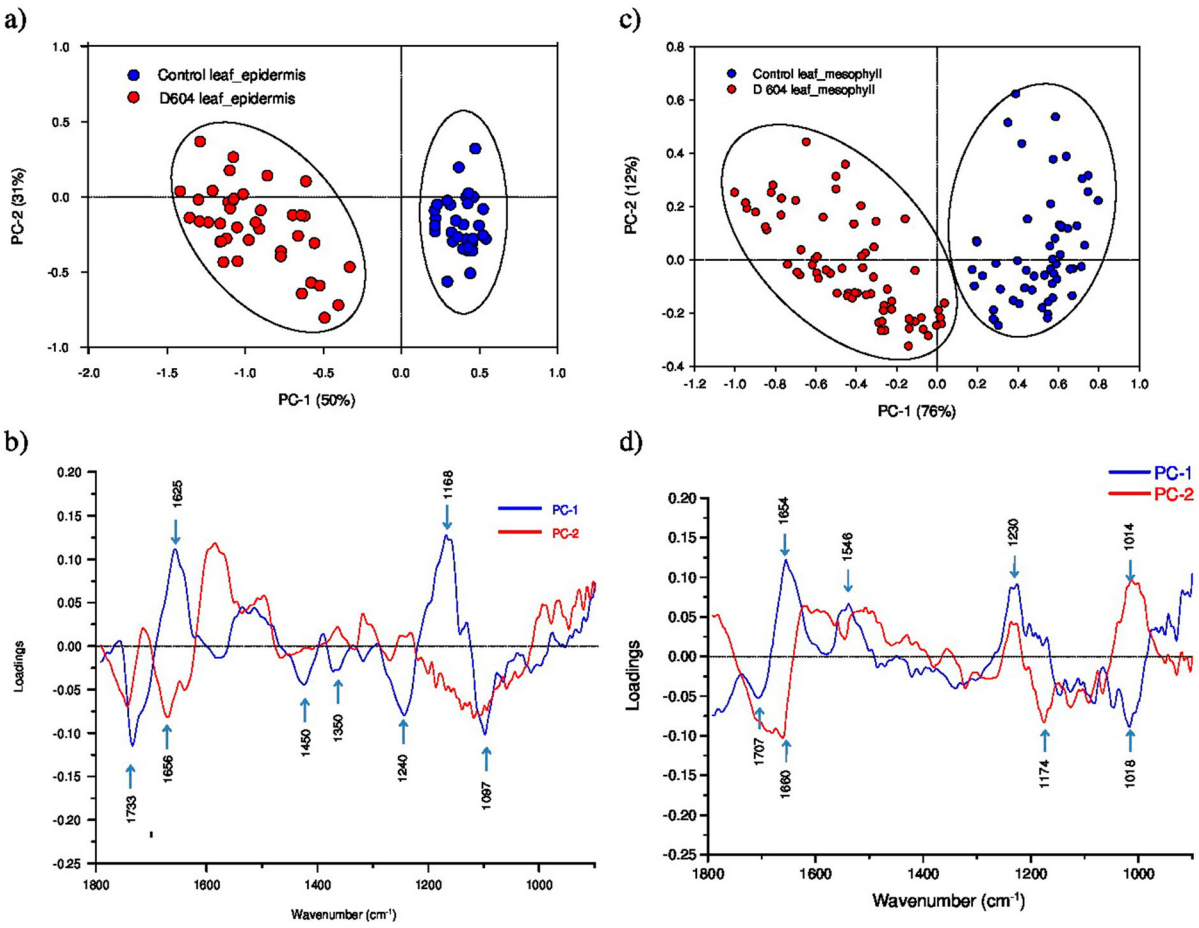

Figure 4. PCA analysis of a chili leaf (a) Score and (b) loading plots from PCA analysis of epidermis control groups compared to treated plants, (c) Score and (d) loading plots from PCA analysis of mesophyll control groups compared to treated plants.

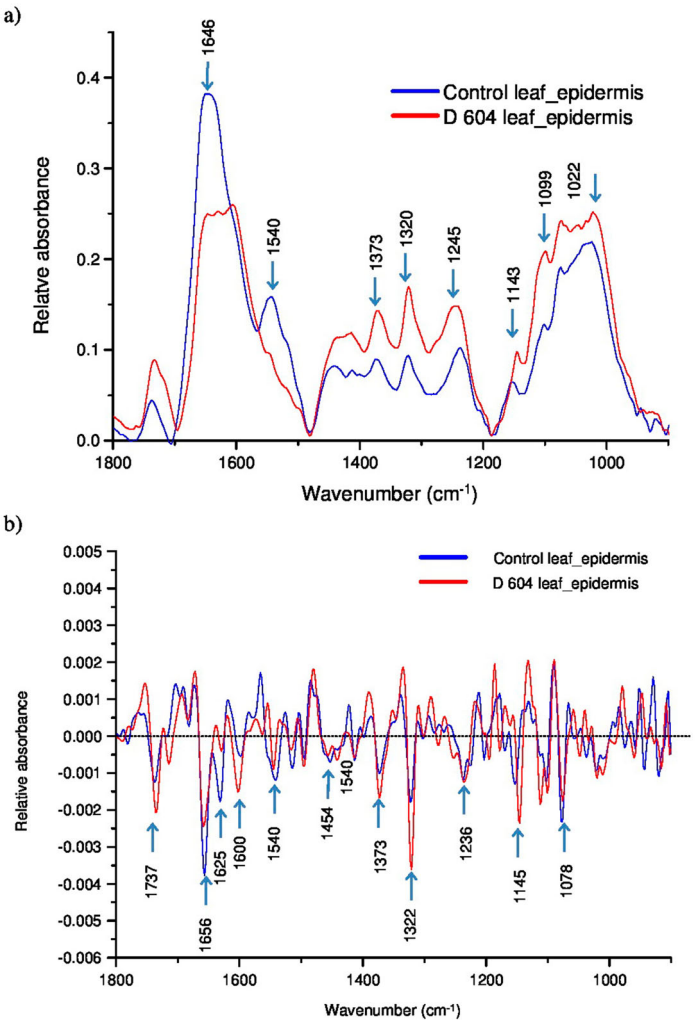

Figure 5. Overlay of the second derivative of the average spectra from a non-treated chili leaf (control) compared with D604-treated chili plants and then challenge inoculation with *C. acutatum*. (a) Epidermis (b) Mesophyll. Average second derivative spectra after 13 points of smoothing and normalization with extended multiplicative signal correction over the spectral range of 1800–900 cm^{-1}.

in both the epidermal and mesophyll tissue regions consistent with alteration of protein structure and cell wall thickening. This study is consistent with studies in cassava in which plant growth-promoting *Bacillus* species elicit the production of plant biological molecules that lead to structural and physiological changes associated with the plant growth and development (Prathuangwong & Buensanteai 2007; Buensanteai et al. 2012; Thumanu et al. 2015).

The epidermal tissues treated with the strain D604 have lower levels of proteins with alpha helix secondary structure and higher levels of proteins with beta sheet secondary structure. Polysaccharides were more abundant in both epidermal and mesophyll regions for leaves treated with D604. The increase of polysaccharides, C=O ester and CH bending for lipid or lignin, Amide I protein in both epidermis and mesophyll leaf tissue likely play an important role in the plant defense (Le Thanh et al. 2017). For example, the biochemical changes may involve enzymes related to the *PAL* gene involving lignin synthesis. The observed alteration of polysaccharide components which induced plant to synthesis some specific compound of defense mechanism pathway against plant disease (Martin et al. 2005; Lahlali et al. 2015). The higher integral areas of CH bending could be related to methoxy phenolic substitution of aromatic units such as syringyl

Table 3. The integral area of average spectra from epidermis of non-treated (control) and treated chili leaf with *Bacillus subtilis* strain D604 and challenge inoculation with *Colletotrichum acutatum*.

	Treatment	
Functional groups	Control	*Bacillus subtilis* strain D604
C=O ester (1740–1700 cm^{-1})	1.10 ± 0.01b	2.36 ± 0.26a
Amide I and Amide II (1700–1500 cm^{-1})	22.23 ± 2.65a	26.97 ± 5.03a
CH bending (1480–1350 cm^{-1})	5.3 ± 0.03b	10.76 ± 1.50a
C–O–C hemicellulose and cellulose (1200–1250 cm^{-1})	2.62 ± 0.40b	4.49 ± 0.29a
C–O, C–C polysaccharide (1200–900 cm^{-1})	22.24 ± 0.41b	34.99 ± 3.24a

Note: Different letters indicate significant differences ($p \leq 0.01$).

Table 4. The integral area of average spectra from a mesophyll of non-treated (control) and treated chili leaf with *Bacillus subtilis* strain D604 and challenge inoculation with *Colletotrichum acutatum*.

	Treatment	
Functional groups	Control	*Bacillus subtilis* strain D604
C=O ester (1740–1700 cm^{-1})	0.51 ± 0.05a	0.77 ± 0.14a
Amide I and Amide II (1700–1500 cm^{-1})	8.92 ± 1.25b	27.98 ± 2.98a
CH bending (1480–1300 cm^{-1})	1.34 ± 0.05a	9.29 ± 1.04a
C–O, C–C polysaccharide (1200–900 cm^{-1})	8.65 ± 1.30b	66.92 ± 10.15a

Note: Different letters indicate significant differences ($p \leq 0.01$).

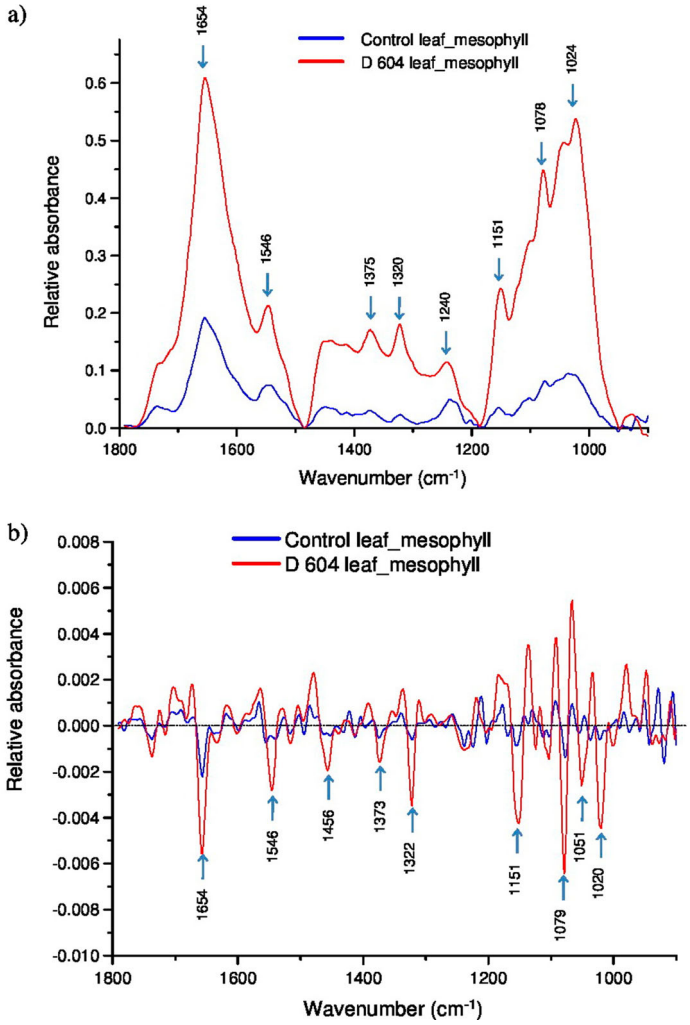

Figure 6. Overlay of the original (a) and second derivative (b) from the average spectra from a chili leaf (control) compared with treated plants from mesophyll tissue. Note: Average second derivative spectra after 13 points of smoothing and normalization with extended multiplicative signal correction over the spectral range of 1800–900 cm^{-1}.

and guaiacyl of lignin. These changes could indicate the formation of lignin and suberin. Lignin is a cell wall component that is covalently linked to hemicellulose and cross-links to different plant polysaccharides. It has a critical effect on the mechanical strength of the cell wall, which plays an important role against many lytic enzymes produced by plant pathogens during host tissue colonization. Integral areas of C=O ester lipid or pectin from the epidermal leaf tissue in the treated group were significantly higher than the control group. This result might imply the accumulation of pectin and polysaccharides in chili associated with cell wall thickening. Plant cell walls are complex composites of cellulose, cross-linking glucans, protein, and pectin substances. The change of alpha helix secondary structure to beta sheet structure in the treated group suggests an important role in cell wall metabolism. For instance, pectin and pectin methyl-esterification are related to plant defense through modification of chemical compositions (Skotti et al. 2014). These biochemical changes may possibly involve enzymes implicated in degradation processes such as pectinases that catalyze de-esterification of pectin by the action of pectin esterferase and other pectin enzymes (Manrique & Lajolo 2004). Interestingly, the peaks in the carbohydrate fingerprint region (1200–1000 cm^{-1}) show an increase in absorbance, particularly in the bands at 1078 and 1145 cm^{-1}. This might be related to pectin polysaccharides, such as homo-galactruonan, rhamnogalacturan, or glucan (callose), known to be found in cell walls of plant leaves (Yu 2005; Dokken & Davis 2007), increasing in response to the strain D604 treatment of the chili plants. The high intensity of alpha helix Amide I structure in the mesophyll leaf tissue of the treated group might be consistent with higher concentrations of enzymes responsible for fixing CO_2 in the chloroplast. The most abundant enzyme in the plant cell responsible for carbon fixation is ribulose bis-phosphate carboxylase/oxygenase, and this protein predominantly has an alpha-helical secondary structure (Heraud et al. 2005). As such, it is possible that the plant has increased levels of photosynthesis in order to support the on-going plant defense response, including reinforcement of the plant cell wall, without greatly reducing the availability of energy devoted to plant growth and development.

Conclusion

SR-FTIR microspectroscopy can be used as a tool to examine the biochemical changes within plant tissue at a high spatial resolution. This technique allows us to reveal the structural chemical makeup of different tissue types. The use of PCA was applied to characterize the spectral differences between epidermal and mesophyll tissues. It can be noted that SR-FTIR microspectroscopy identified biochemical and structural changes of chili that help us to understand the mechanisms of

plant defense induced by PGPR. In particular, chili treated with the strain D604 produced leaves that displayed changes in SR-FTIR spectra from epidermis and mesophyll tissue regions that may be associated with compositional and concentration changes of proteins, lipids, pectins, and polysaccharides. Therefore, this study suggests that the structural changes of the plant epidermal and mesophyll cells could be induced by the *B. subtilis* strain D604 and the anthracnose fungal pathogen in chili pepper. In the future, we plan to collect leaf samples at differing harvest times in order to compare spectral differences that could be occurring during the resistance mechanism of chili. This information will help us to understand the relationship between plant growth regulators and yield improvement.

Acknowledgments

The authors would like to thank the Dr Sopone Wongkaew and Mr Michael Greene for all suggestions and valuable comments. The authors wish to express their special thanks to Plant Pathology Laboratory, Suranaree University of Technology, and to graduate students and research assistant for the technical assistance. They would also like to thank the Synchrotron Light Research Institute (Public Organization) for providing the FTIR instruments and beam times.

Disclosure statement

No potential conflict of interest was reported by the authors.

Funding

This work was supported by Suranaree University of Technology; the Higher Education Research Promotion and National Research University Project of Thailand, Office of the Higher Education Commission. The acknowledgement is also extended to the Research and Researcher for Industries (RRi), the Thailand Research Funds [grant number MSD57I0118] to Miss Darawadee Wongchalee.

References

Ashwini N, Srividya S. 2014. Potentiality of *Bacillus subtilis* as biocontrol agent for management of anthracnose disease of chili caused by *Colletotrichum gloeosporioides* OGC1. Biotechnology. 4:127–136.

Buensanteai N, Thumanu K, Sompong M, Athinuwat D, Prathuangwong S. 2012. The FTIR spectroscopy investigation of the cellular components of cassava after sensitization with plant growth promoting rhizobacteria, *Bacillus subtilis* CaSUT007. Afr J Microbiol Res. 6(3):603–610.

Buensanteai N, Yuen GY, Prathuangwong S. 2008. The biocontrol bacterium *Bacillus amyloliquefaciens* KPS46 produces auxin, surfactin and extracellular proteins for enhanced growth of cucumber plant. Thai J Agric Sci. 41:101–116.

Buensanteai N, Yuen GY, Prathuangwong S. 2009. Priming, signaling, and protein production associated with induced resistance by *Bacillus amyloliquefaciens* KPS46. World J Microbiol Biotechnol. 25:1275–1286.

Conrath U, Beckers GJM, Flors V, García-Agustín P, Jakab G, Mauch F, Newman M, Pieterse CMJ, Poinssot B, Pozo MJ, et al. 2006. Priming: getting ready for battle. MPMI. 19:1062–1071.

Dokken KM, Davis LC. 2005. Use of infrared microspectroscopy in plant growth and development. App Spectrosc Rev. 40:301–326.

Dokken KM, Davis LC. 2007. Infrared imaging of sunflower and maize root anatomy. J Agric Food Chem. 55:10517–10530.

Heraud P, Caline S, Sanson G, Gleadow R, Wood BR, McNaughton D. 2005. Focal plane array infrared imaging: a new way to analyse leaf tissue. New Phytol. 173:216–225.

Kenneth MD, Lawrence CD. 2005. Use of infrared microspectroscopy in plant growth and development. Appl Spectrosc Rev. 40:301–326.

Kloepper JW, Ryu CM, Zhang SA. 2004. Induced systemic resistance and promotion of plant growth by *Bacillus* spp. Phytopathol. 94:1259–1266.

Lahlali R, Karunakaran C, Wang L, Willick I, Schmidt M, Liu X, Borondics F, Forseille L, Fobert PR, Tanino K, et al. 2015. Synchrotron based phase contrast X-ray imaging combined with FTIR spectroscopy reveals structural and biomolecular differences in spikelets play a significant role in resistance to Fusarium in wheat. BMC Plant Biol. 15:1–24.

Le Thanh T, Thumanu K, Wongkaew S, Boonkerd N, Teaumroong N, Phansak P, Buensanteai N. 2017. Salicylic acid-induced accumulation of biochemical components associated with resistance against *Xanthomonas oryzae* pv. *oryzae* in rice. J Plant Interact. 12:108–120.

Manrique GD, Lajolo FM. 2004. Cell-wall polysaccharide modifications during postharvest ripening of papaya fruit (*Carica papaya*). Posth Biol Technol. 33(1):11–26.

Martin AJ, Solla A, Woodward S, Gil L. 2005. Fourier transform-infrared spectroscopy as a new method for evaluating host resistance in the Dutch elm disease complex. Tree Physiol. 25:1331–1338.

Pakdeevaraporn P, Wasee S, Taylor PWJ, Mongkolporn O. 2005. Inheritance of resistance to anthracnose caused by *Colletotrichum capsici* in *Capsicum*. Plant Breed. 124: 206–208.

Plodpai P, Chuenchit S, Petcharat V. 2008. Biocontrol of some chili fungus diseases by *Bacillus* spp. Agricultural Sci J. 39: 185–188.

Prathuangwong S, Buensanteai N. 2007. *Bacillus amyloliquefaciens* induced systemic resistance against bacterial pustule pathogen with increased phenols, peroxides, and 1, 3-β-glucanase in soybean plant. Acta Phytopathol et Entomol Hungarica. 42:321–330.

Ryu CM, Murphy JF, Mysore KS, Kloepper JW. 2004. Plant growth-promoting rhizobacteria systemically protect *Arabidopsis thaliana* against Cucumber mosaic virus by a salicylic acid and NPR1-independent and jasmonic acid-dependent signaling pathway. Plant J. 39:381–392.

Skotti E, Kountouri S, Bouchagier P, Tsitsigiannis DI, Polissiou M, Tarantilis PA. 2014. FTIR spectroscopic evaluation of changes in the cellular biochemical composition of the phytopathogenic fungus *Alternaria alternate* induced by extracts of some Greek medicinal and aromatic plants. Spectrochim Acta A Mol Biomol Spectrosc. 127: 463–472.

Thumanu K, Sompong M, Phansak P, Nontapot K, Buensanteai N. 2015. Use of infrared microspectroscopy to determine leaf biochemical composition of cassava in response to *Bacillus subtilis* CaSUT007. J Plant Interact. 10:270–279.

Wang J, Zhuac J, Huangac RZ, Yang Y. 2012. Investigation of cell wall composition related to stem lodging resistance in wheat (*Triticum aestivum* L.) by FTIR spectroscopy. Plant Signaling Behav. 7:856–863.

Yu P. 2005. Molecular chemistry imaging to reveal structural features of various plant feed tissues. J Struct Biol. 150:81–89.

Yu P. 2008. Synchrotron-based microspectroscopic analysis of molecular and biopolymer structures using multivariate techniques and advanced multi-component modeling. Can J Anal Sci Spectrosc. 53:220–231.